THE UNIVERSITY OF MICHIGAN

College of Engineering

Department of Mechanical Engineering

Cavitation and Multiphase Flow Laboratory

Report No. UMICH-324490-2-T

LIQUID IMPINGEMENT AND CAVITATION STUDIES OF EROSION RESISTANCE OF RUBBER-COATED MATERIALS FOR B. F. GOODRICH

by

F. G. Hammitt

E. E. Timm

J. B. Hwang

Y. C. Huang

May, 1972

TABLE OF CONTENTS

Page

LIST OF FIGURES

LIST OF TABLES

ABSTRACT

High-speed motion picture sequences of liquid jet impact at 500 MPH with 7 rubber-coated materials supplied by B.F. Goodrich have been obtained, showing in good detail the portion of the impact believed responsible for damage. Some conclusions on favorable characteristics of the splash pattern for superior damage resistance are made.

The erosion resistance of the same materials has been measured with repeated impacts with the same type of water jet at the same velocity. Pertinent information from related numerical studies of droplet impact supported by NSF are here included.

I. INTRODUCTION

The second year of a contract between B. F. Goodrich Co. and the Cavitation and Multiphase Flow Laboratory of the Mechanical Engineering Department of the University of Michigan had a two-fold objective:

1. Obtain high-speed motion pictures of the impacts of ~500 MPH water jets generated by our water gun device upon 7 rubber-coated materials supplied by Goodrich to observe the details of such collision, and attempt to ascertain possible differences in the response of materials that might be related to their droplet impact erosion resistance. The framing rates for these pictures should be such that as many frames as possible be available during the critical part of the impact process. The pictures (Fig. 3-9) were taken with our Beckman-Whitley framing camera capable of producing up to 80 frames per run at 2 million frames per second. Due to the short time which can be sampled, optimum information in this case is obtained with less than maximum framing rate. Fig. 1 and 2 show the water gun, light source, and related equipment.

2. Measure resistance to liquid impact erosion of the same materials using our water gun device, and attempt to relate their resistance to the splash patterns obtained from the camera. Damage results are tabulated in Table 1.

All of the above tasks have been completed as explained in the body of the report. These results suggest to us the desirability of additional investigations covering another year of effort, as will also be explained later.

1

II. PHOTOGRAPHIC AND EXPERIMENTAL OBSERVATIONS

A. Experimental Facilities Utilized

1. Impact Facility. While the facilities were described in our previous report (1), the important points are repeated here for convenience. For the liquid jet impact tests, a repeating water gun (Fig. 1 and 2) was utilized.[1] This device produces liquid jets with velocity up to about 600 m/s, emanating from an orifice of 1.6. mm. dia. The repetition rate is about 50 per minute. The actual jet shape depends upon various parameter settings. For the present tests, wherein the impact velocity was 223 m/s (500 MPH) its appearance is as shown in Fig. 3-9. The portion of the impact shown (up to 80 μs) is with a "precursor jet" of diameter 1/3 mm which is somewhat smaller than diameter of the main jet (1.2 mm). It is believed that the damaging part of the impact is the initial part during which high transient pressures and velocities are possible. The pressure and velocity across the surface of a "steady-state" jet of the present impact velocity would be much smaller and probably not damaging during the short time of the collision.

The seven rubber-coated materials supplied by B.F. Goodrich (Table 1) were with angle of impact perpendicular. Photographic sequences of the collisions were then obtained (Fig. 3-9) using our high-speed framing camera. Damage tests were then made for all these materials with repeated impact under the conditions for which the photographs were made (Table 1).

2. High Speed Motion Picture Facility. The motion picture sequences of the water jet impacts (Fig. 3-9) were made with a Beckman-Whitley framing camera capable of a maximum framing rate of 2 million frames/second, with a total of 80 frames/run. To obtain maximum information per run, a framing rate of 0.5 million frames per second was used.

2

As will be observed in Fig. 3-9, it is quite possible to estimate the radial and axial velocities of the liquid during the collision utilizing the times from initial impact noted on the individual photos. Though this was done in the previous tests (1), it has not been done as yet for the present data. Note also that the flow patterns are well-developed by about 40 μs, and that there are considerable differences in flow patterns generated between the materials. Unfortunately, it is not possible in these photos to observe the deflection of the specimen surface during the impact. However, from the steep angle of splash-back, it may be inferred that in some cases this deformation is considerable. Possible methods for measuring the deformation during the impact and correlating it to photos such as these is discussed later in the report.

B. Liquid Impact Photographic Results

Fig. 3-9 respectively show high-speed motion picture sequences of impacts of 500 MPH (732 f/s = 223 m/s = 0.67 Mach at STP for the materials suppled by Goodrich. The times in microseconds from initial impact are shown in each frame. Though approximately 80 frames were exposed per run, only selected frames are shown to indicate the significant features of the impact. The portion of the overall impact shown by the figures is that with the "precursor" portion of the main jet which has a diameter of about 1/3 mm., and persists up to about 80 μs. The main jet of about 1.2 mm diameter follows, but since this latter portion of the collision is a roughly steady-state impingement, as compared to the first portion, it is not thought to be important to the damage process. Our numerical calculations (2, 3, 4, e.g.) to be briefly explained later, indicate that the damaging pressures and maximum velocities should persist only during the 1st μs after collision with "steady-state" conditions being closely approached after a few microseconds.

As indicated in our previous report(1), though the impact phenomenon is quite similar for all the materials, significant differences in the velocity and direction of splash-back were indicated. This splash-back was minimal for the more rigid materials then tested (1) (Epon and Plexiglas), and quite

3

pronounced in all of the rubber-coated materials, (except for the natural rubber Goodrich #1 which appeared similar in this respect to the rigid materials). The numerical data for the present tests have not been calculated as yet, though this could be done in follow-on work. In general, the splash patterns for the present materials (Table 1) appear quite similar to those for the resilient materials tested previously (1), and quite similar to each other.

However, splash-back is minimal for materials Goodrich #923 and #936 (similar to more rigid materials as Epon and Plexiglas), but maximum for Goodrich #932, although the resistance to impact is relatively similar for these materials and much less than for Goodrich A, B, C, and D. In those cases where splash-back is minimum, radial velocity and spreading along the surface appears to be maximum. There was no visible change of surface texture during the tests until a small straight crack developed. This was the mode of failure of all the specimens. Fig. 10-a illustrates such an initial crack. The number of impacts to the first appearance of such a crack is tabulated in Table 1.

III. EROSION OBSERVATIONS

A. Impact Erosion Tests

The 7 elastomeric-coated Goodrich materials have been tested at the same velocity for which the impact photographs were taken (223 m/s). The results, in terms of number of impacts to failure, are listed in Table 1. It was found to be impossible to measure weight losses during these tests because of the proclivity of the specimens to absorb moisture.

The tests are conducted with incremental numbers of impacts between observations. Since the approximate required number of impacts was not known in advance, the increments between observations were sometimes longer than desirable. Thus the precise number of impacts to the first appearance of a crack is known only within a range which, however, is small (Table 1) compared to the difference in number of impacts between different specimens. The first column in Table 1 lists number of impacts

4

corresponding to the last observation of the specimen before any surface failure was visible. The second column shows number of impacts corresponding to the first observation after a surface failure was noted. The third column is the average of the first two, and this gives the most probable number of impacts to surface failure. In some cases no failure was noted up to 20,000 impacts,[*] which was felt to be the maximum number feasible within the present contract. The unfailed specimens could of course be tested to eventual failure under a follow-on contract.

Since two specimens of material #932 were available, both were tested. Whereas the number of impacts to failure differs by a factor of about 6 between these specimens of the same material, the average for all the numbered material specimens is within a range of about $\pm$ 10%. These are all thus somewhat better than material A, but very much worse than materials B, C, and D (factor of at least 4).

Figure 10-b shows the continued mode of failure after the initial appearance of a crack (specimen#932-2),showing a larger failure area with small radial cracks outward from the central failed area, This photo corresponds to 2600 impacts, i.e. 600 impacts beyond the initial failure.

Examination of the impact photos (Fig. 3-9) shows that those of the most resistant materials (B, C, and D) each produce a relatively very substantial splash-back. However, this is also true of specimen A which was least resistant of all materials tested (with the exception of one specimen of material #932) and was worse than the average for any other material. Of the numbered materials, only #932 shows a substantial splash-back. It was noted in our previous tests (1), that a large splash-back appeared to be desirable for good erosion resistance. It thus appears in general that this feature of the impact behavior tends to correlate with good erosion resistance , but that other material parameters are also involved and give opposing trends which

---

[*]A small circular blemish of the surface was noted. However, this was too faint to be shown photographically.

sometimes apparently control. Large splash-back would appear to indicate large surface resiliance and deformation under impact. Additional research to measure surface deformation and pressures generated upon the surface appears to be desirable to obtain further understanding of those parameters of the material leading to good erosion resistance.

B. Numerical Studies

Various numerical studies of the impact process have been made in this laboratory under related work supported by the National Science Foundation (2,3,4, e.g.), primarily as the Ph. D. thesis of Y. C. Huang, now completed. These on-going studies have shown that the important events from the viewpoint of damage, for droplet sizes and velocities here considered, occur during the first 1-2 μs after impact. The maximum pressures depend upon droplet leading-edge shape, and only slightly upon droplet length. For realistic leading-edge shape, the pressure is somewhat less than the "water-hammer pressure"*, even if this is uncorrected for the increased shock-wave velocity under impact conditions. These results for rigid flat targets are summarized in Table 2.

A preliminary calculation has also been made (4) for an elastic surface (including only inertial resistance to deformation). Work toward the development of a more comprehensive computer code for resilient surfaces is underway now as a new Ph. D. thesis. Fig. 11 shows the droplet and target surface profiles, and pressure isobars in the liquid, for impact of an initially spherical droplet upon an initially flat surface characterized by an acoustic impedance equal to that of water, at a time about 1.23 μs after impact for a 1.5 mm. diameter drop impacting with 250 m/s velocity from our preliminary calculations (4). The surface deformations are greatest under an annulus near the outer contact area. This is consistent with damage patterns observed on Plexiglas (5, e.g.) impacted by spherical water droplets where a failure annulus occurs at approximately this location.

*$P = \rho_o C_o V$, where ρ_o = unperturbed liquid density, C_o = sonic velocity in liquid
V = impact velocity.

The maximum pressure developed[*]is no doubt less for the resilient surface than for the rigid surface. However, numerical results for these pressures are not yet available.

IV. RECOMMENDED FUTURE WORK

Obviously the work so far completed is only a beginning in many areas, so that desirable and significant new work can be postulated. Possible areas of major importance are suggested below.

A. Detailed Material Response to Liquid Impact

A complete understanding of the material response under liquid impact, and the mechanisms leading to initial failure, would allow a more rational design of more resistent materials. The presently completed tests show in detail the motion of the water during the significant portion of the impact from the viewpoint of damage for a variety of materials. However, it is not possible to view the motion of the surface during this time. It is possible to infer an estimate of this motion from the fluid motion observed in the photos. This involves a rather intricate and lengthy analysis which has not yet been done, but we believe should be included in follow-on work. The continuation of computerized calculations of velocity and pressures on the surface of rigid and deforming surfaces during impact should allow the predication of these splash velocities and a check of the analysis against the present photographs. This essentially analytical approach is being continued under NSF support. However, further significant experimental information should be sought as explained below.

It is possible to measure surface motion during impact using laser interferometry with a transparent surface. A facility which could be used for this purpose already has been developed here in connection with another project, and could be applied to measurements of the motion of a surface under droplet impact. The initial set-up would involve a transparent target/material as Plexiglas with a silvered surface upon which droplet impact would occur. Such measurements would allow the check of our numerical code, which would then be applied to non-transparent surfaces of any given properties.

8

It is also possible that instantaneous pressures can be measured on the surface, although the state of the art of transducers indicates that considerable development would be required.

B. Prevention or Reduction of Cavitation Damage by Surface Flexibilty

It is theoretically expected and has been shown by past tests, some of which were just recently completed in this laboratory (6), that, while a rigid surface will attract a collapsing bubble and cause the orientation of the resultant microjet to be toward the surface, the inverse is the case with a sufficiently flexible surface, so that cavitation bubbles are actually repelled, and the microjet oriented away from the surface of the material. Thus a material with a suitably-designed flexible surface might be virtually immune to cavitation damage. Preliminary tests (6), which we have completed with spark-induced bubbles collapsing adjacent to a rubber diaphram stretched across an air space, indicate that the theoretically postulated mode of collapse described above actually occurs. Hence, a further investigation of this phenomenon using our relatively unique high-speed photographic facilities with tests in both our venturi and beaker set-ups could point the way to the rational design of rubberized materials to take advantage of this facet of bubble dynamics.

C. Additional Tests of Material Resistance

Additional tests could involve any combination of different materials, velocities, impact angle, duration, environmental conditions of target temperature or ambient pressure. They could be either of the impact or cavitation type.

V. CONCLUSIONS

The major conclusions which can be drawn from this work follow.

1. Detailed motion pictures of the impact from the water gun jet at~500 MPH upon 7 elastomer-coated materials supplied by Goodrich have been made. Observed differences in splash-back and radial velocities have been discussed. The characteristics of the splash differ considerably between these materials. It appears in general, consistent with our previous results (1), that large splash-back and hence reduced radial spreading correlates postively with erosion resistance. However, there are exceptions indicating that other factors too are involved. Even with the same material, there appears to be very large differences between specimens in erosion resistance.

2. The experimental results here obtained can be better understood when considered along with numerical results we are obtaining under NSF sponsorship (some herein presented) of droplet behavior during impact. Hence, a continuation of this relatively modest experimental program will allow a more rapid gain toward rational design of materials for erosion resistance than would be possible for this small program alone. Avenues for follow-on work are suggested in the report.

ACKNOWLEDGEMENT

VI. BIBLIOGRAPHY

1. Hammitt, F. G. , et. al. , "Liquid Impingement and Cavitation Studies of Erosion Resistance of Rubber-Coated Materials for B. F. Goodrich, "; ORA Report No. UMICH 324490-1-T, Univ. of Mich, 1970.

2. Huang, Y. C. , "Numerical Studies of Unsteady, Two-Dimensional Liquid Impact Phenomena, " PhD Thesis, the University of Michigan, 1971; also available as ORA Report No. UMICH 033710-8-T, 1971.

3. Huang, Y. C. , Hammitt, F. G. , Yan , W-J. , "Hydrodynamic Phenomena During High Speed Collision Between Liquid Droplet and Rigid Plane, " ; also available as ORA Report No. UMICH 03371-12-T, 1972, submitted ASME.

4. Hammitt, F. G. , Huang, Yen C. , "Liquid Impact on Elastic Solid Boundary, "; ORA Report No. UMICH 03371-12-T , 1972.

5. Brunton, J. H. , "High Speed Liquid Impact, " Phil. Trans. , Roy. Soc. , A, 1110, 260 , July 1966, 78-85.

6. Timm, E. E. , Hammitt, F. G. , "Bubble Collapse Adjacent to a Rigid Wall, a Flexible Wall, and a Second Bubble, " ; ORA Report No. UMICH 033710-8-I, 1971; also 1971 ASME Cavitation Forum, 18-20.

TABLE 1

JET GUN TESTS OF GOODRICH MATERIALS

Specimen	No. of Impingement (before first appearance of crack)		Average
923-1	4000-5000		4500
932-1	9400-9500)		5600
932-2	1500-2000		
936-1	5100-5200		5150
		Average	5083
A	3400-3500		3450
B	No crack at 20,000		> 20,000
C	No crack at 20,000		> 20,000
D	No crack at 20,000		> 20,000

3429

TABLE 2

Summary of Principal Numerical Results

	M = 0.2 (V_o = 300 m/s)			M = 0.5 (V_o = 750 m/s)		
	$\dfrac{Pmax}{\rho_o C_o V_o}$	$\dfrac{Pmax}{\rho_o CV}$	$\dfrac{Vmax}{V_o}$	$\dfrac{Pmax}{\rho_o C_o V_o}$	$\dfrac{Pmax}{\rho_o CV_o}$	$\dfrac{Vmax}{V_o}$
Free Slip Wall Boundary						
$\dot{m}$	1.17	0.84	2.00	1.61	0.82	1.65
$\dot{m}$	0.69	0.495	2.65	1.07	0.52	2.15
$\dot{m}$	0.90	0.65	2.80	1.30	0.66	2.25
Non-Slip Wall Boundary						
$\dot{m}$	1.20	0.87	2.10	1.675	0.85	1.70
$\dot{m}$	0.80	0.59	2.85	1.229	0.625	2.30

$$\rho_o C_o V_o = \rho_o V_o^2 / M = \qquad 4450 \text{ bars} \qquad\qquad 11,100 \text{ bars}$$

3428

Experimental Arrangement
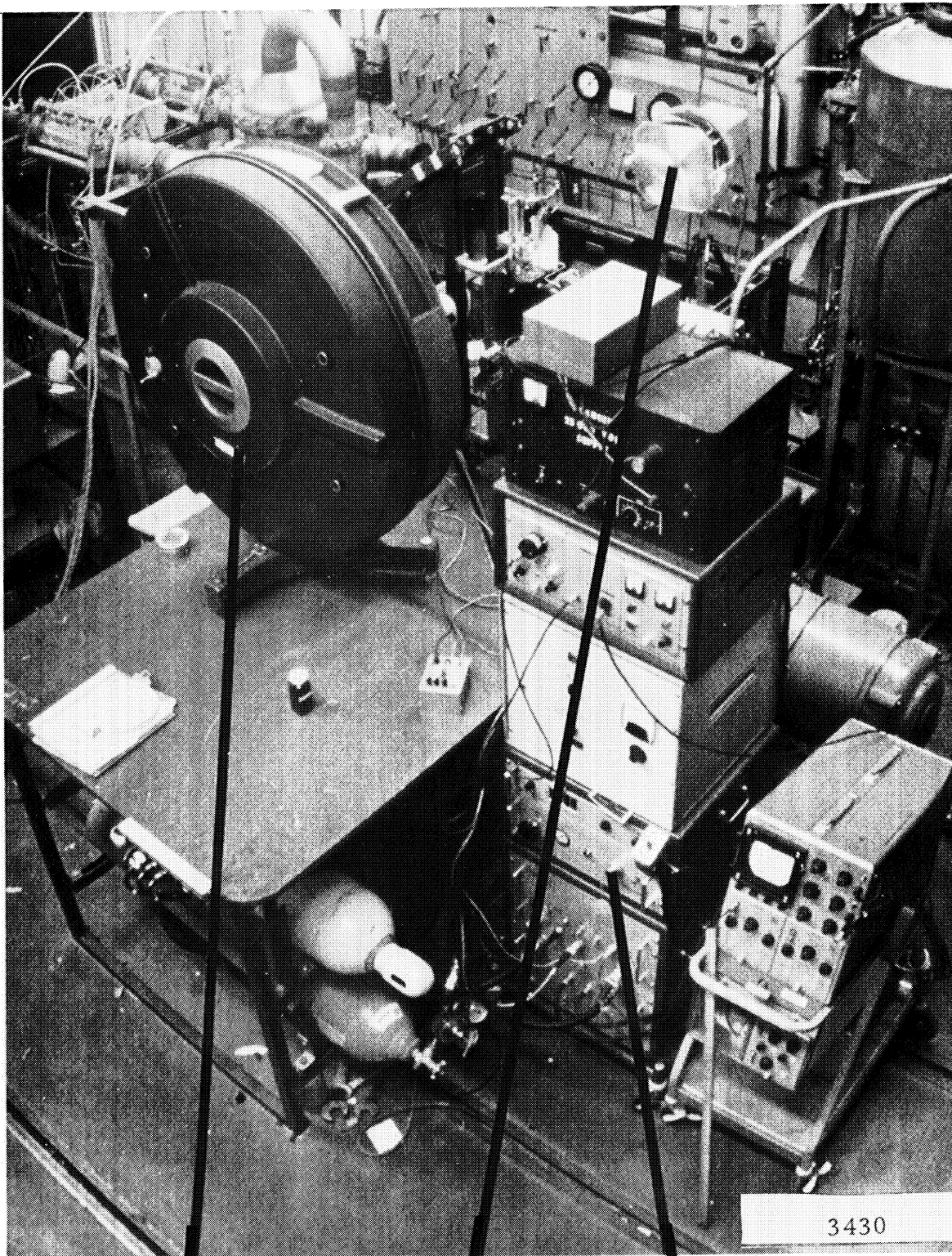
Camera   Light Source   Camera Controls

Figure 1   Experimental Arrangement

Closeup of
Experimental Arrangement
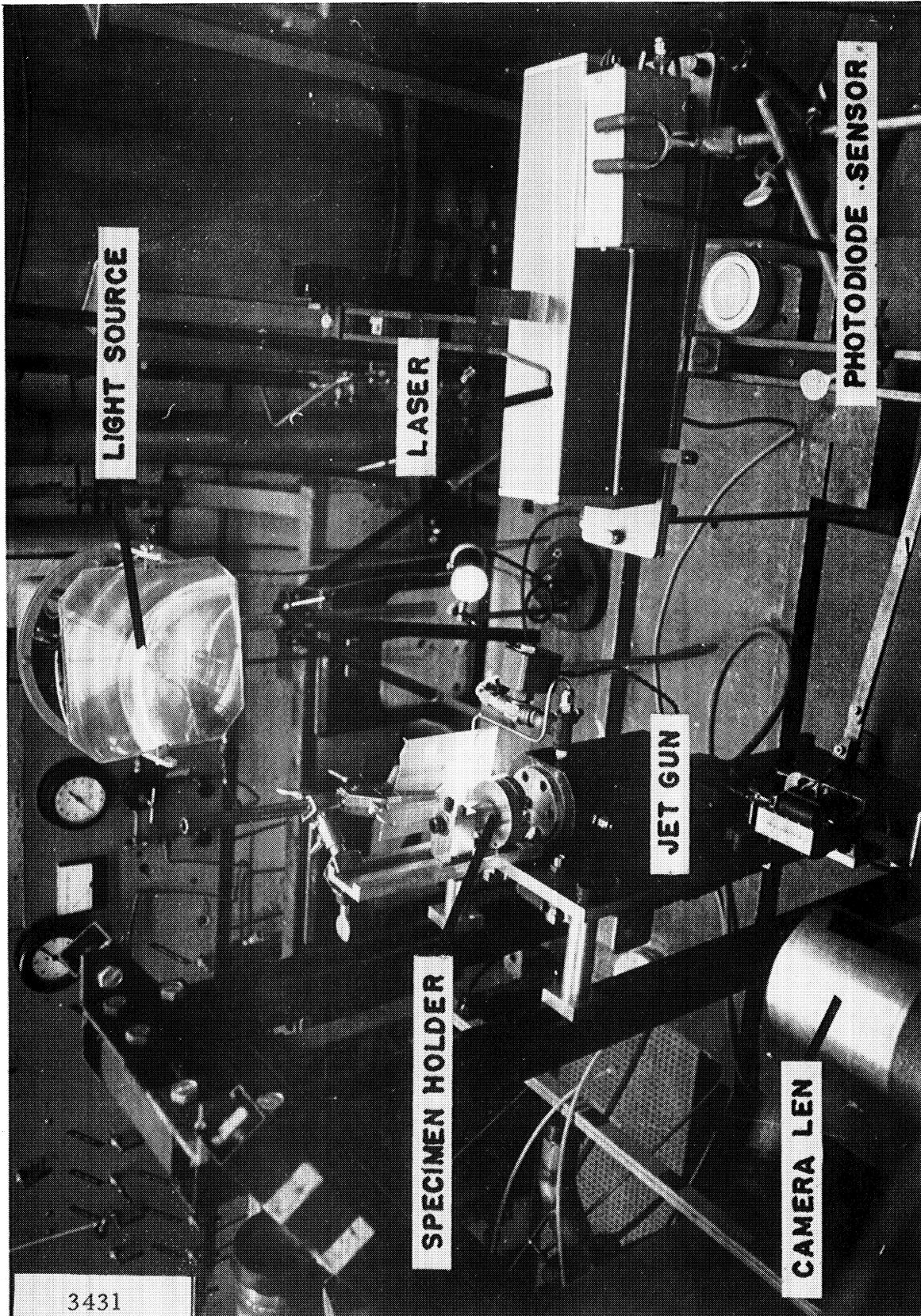
Figure 2 Close-up of Experimental Arrangement

LIGHT SOURCE

LASER

PHOTODIODE SENSOR

JET GUN

SPECIMEN HOLDER

CAMERA LEN

3431

Goodrich 923

t = 10 μs

t = 20 μs

t = 30 μs
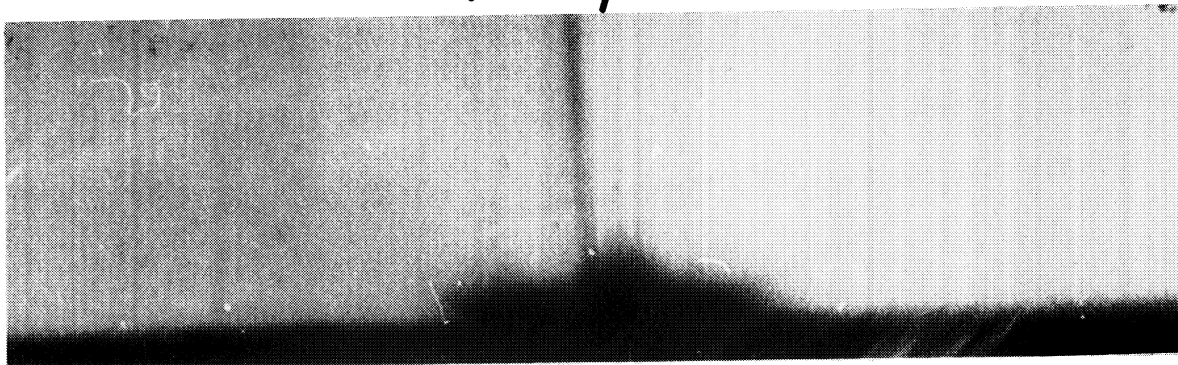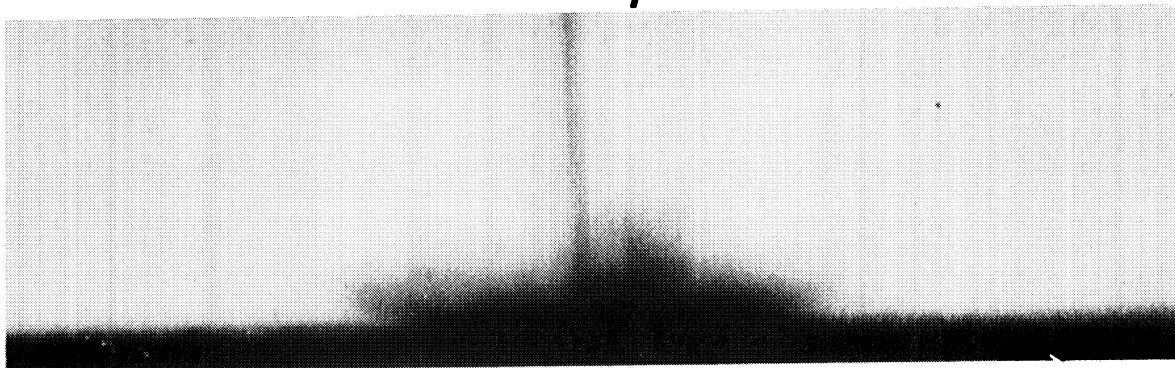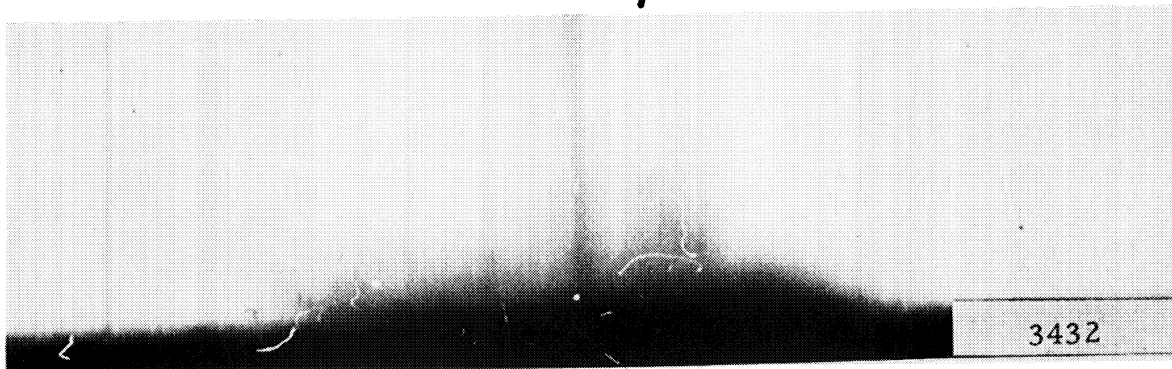
t = 40 μs

Figure 3. High-Speed Motion Picture Sequence of Jet
Impact - Goodrich # 923

16

t= 50 μs

t= 60 μs

t= 70 μs

3433
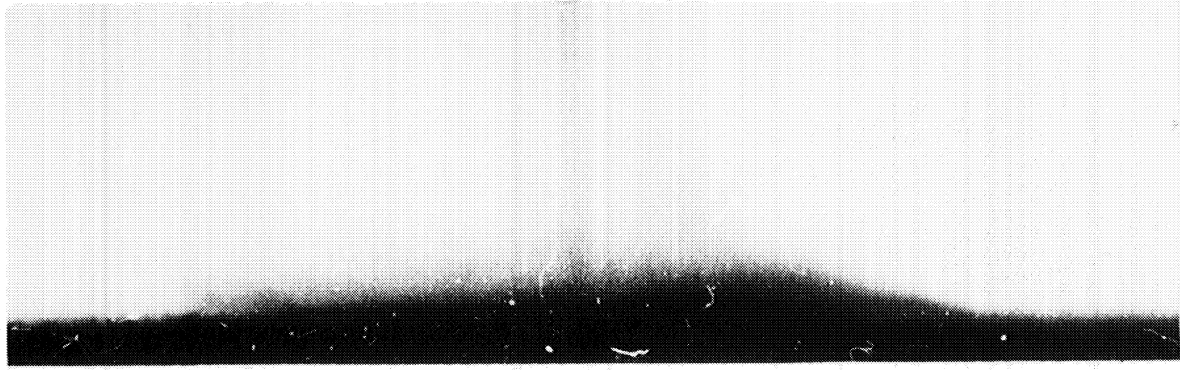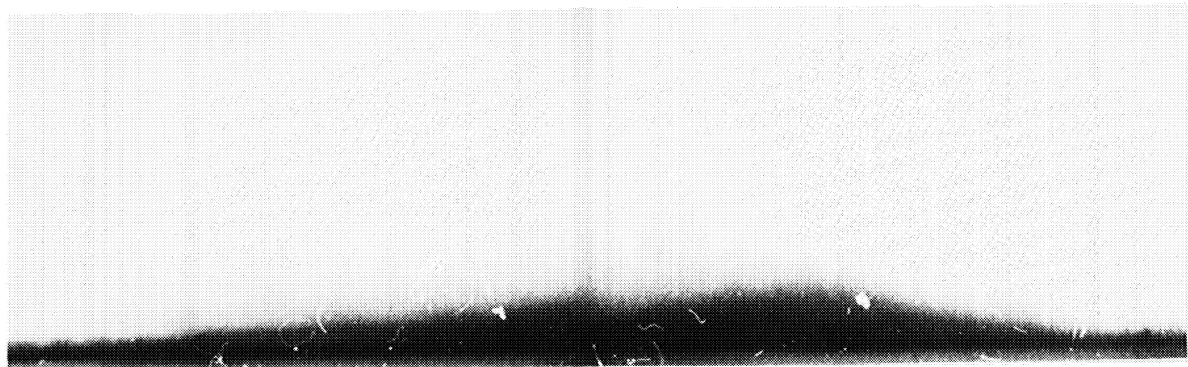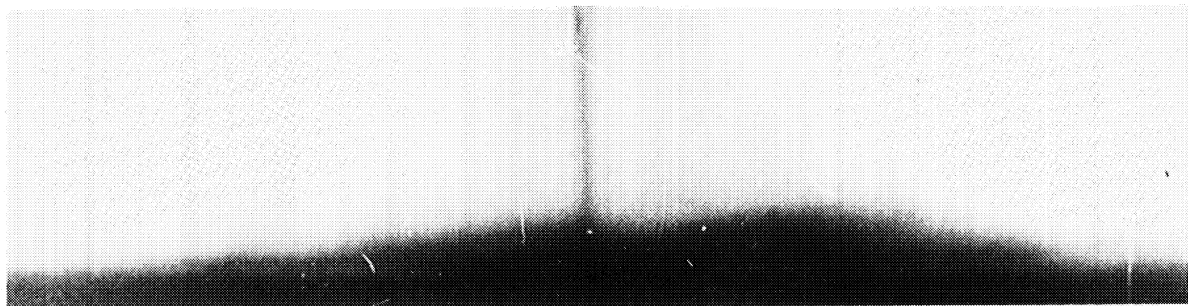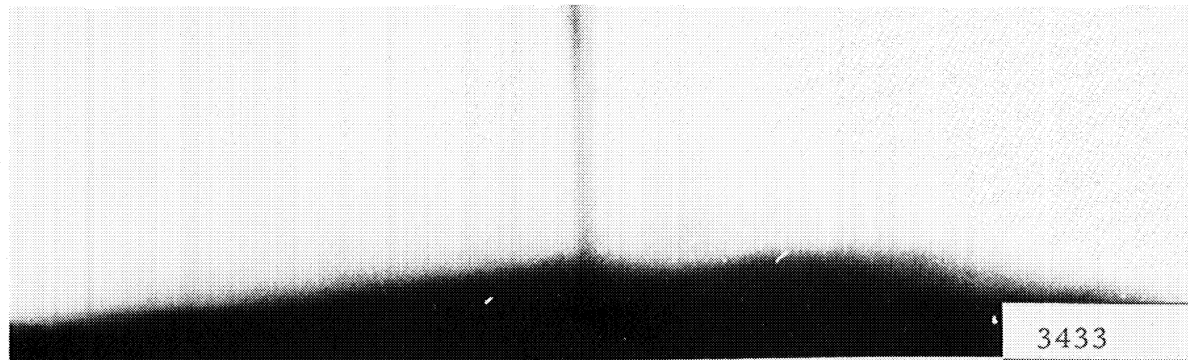
t= 80 μs

Figure 3. (Concluded)
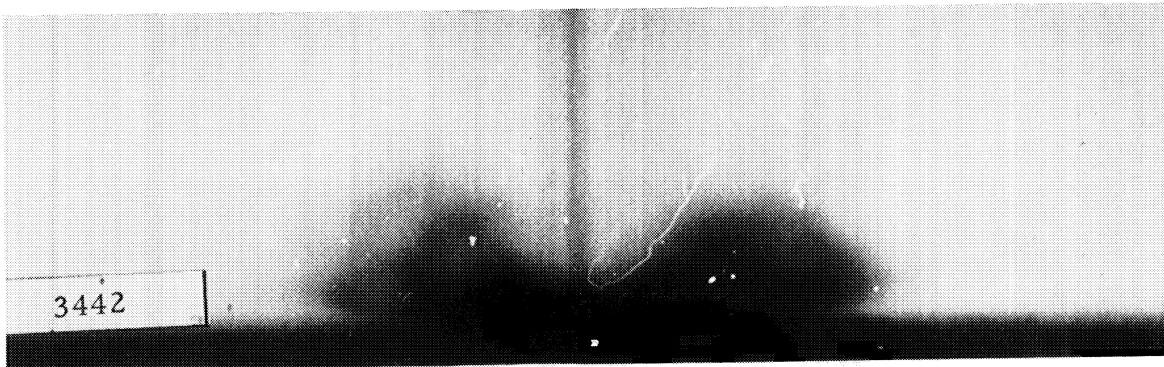
Goodrich 932
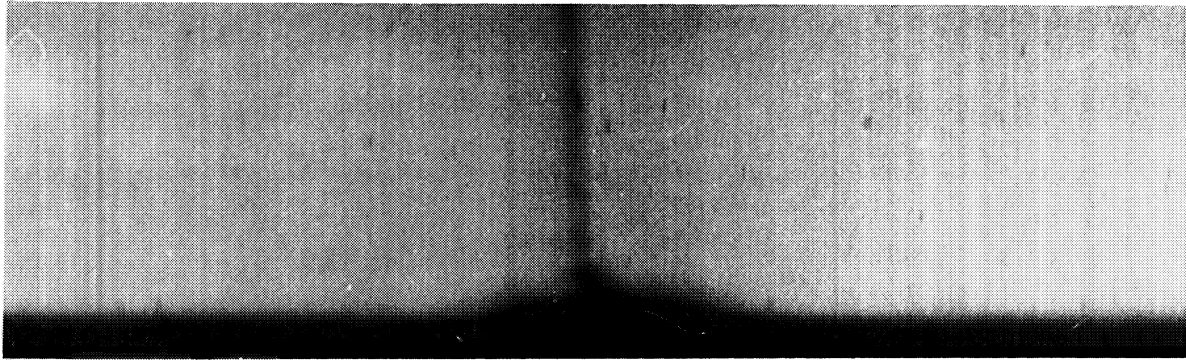
$t = 10 \, \mu s$
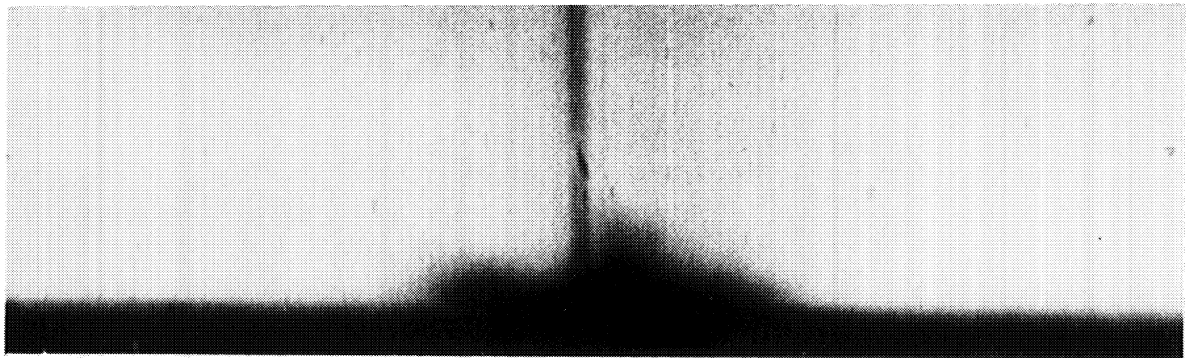
$t = 20 \, \mu s$
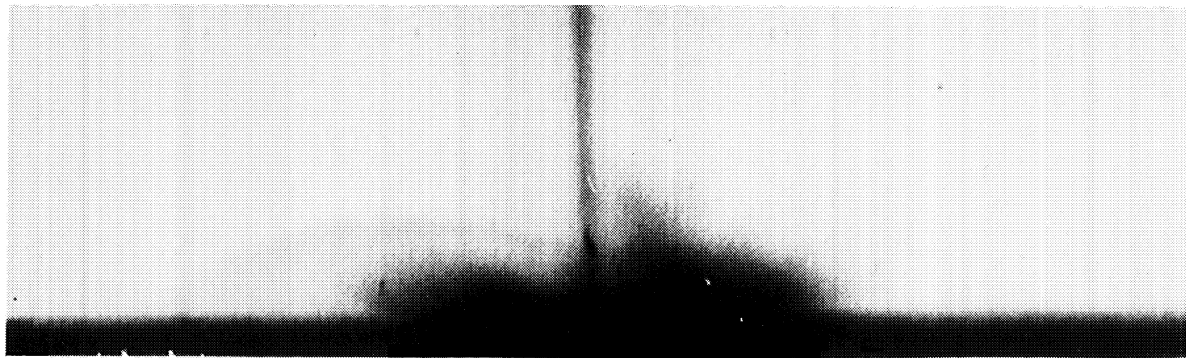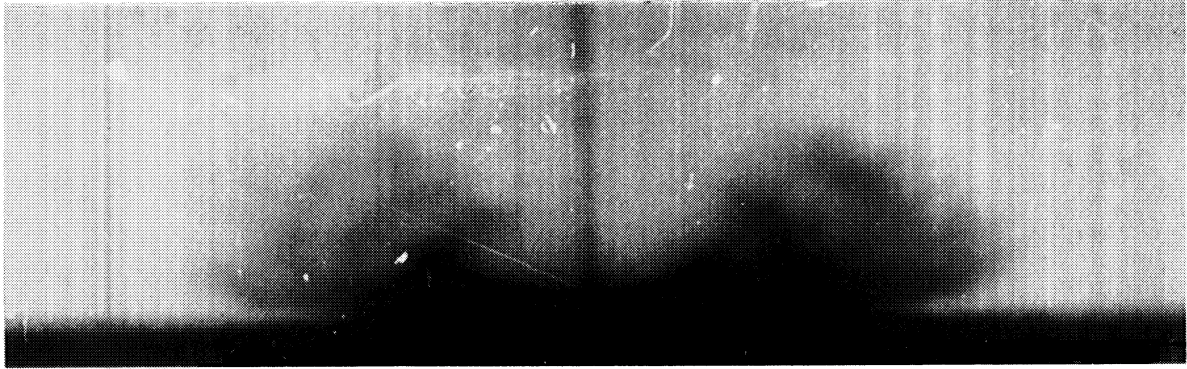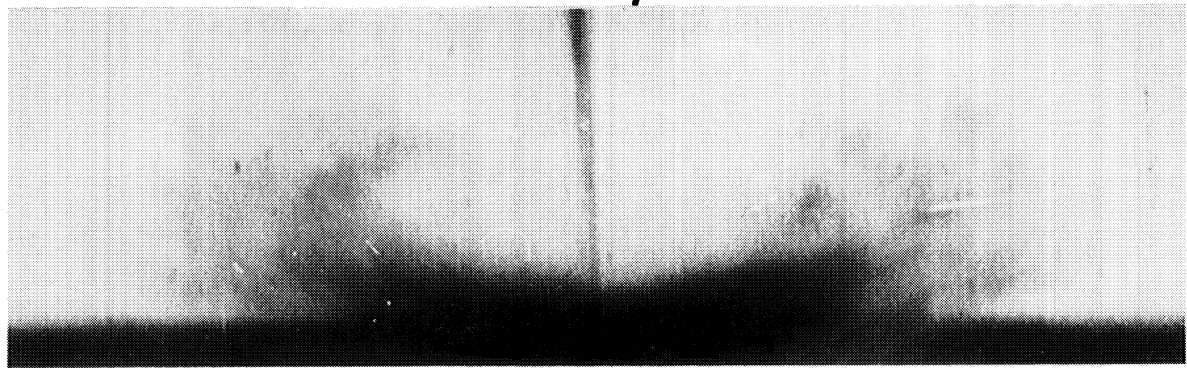
$t = 30 \, \mu s$
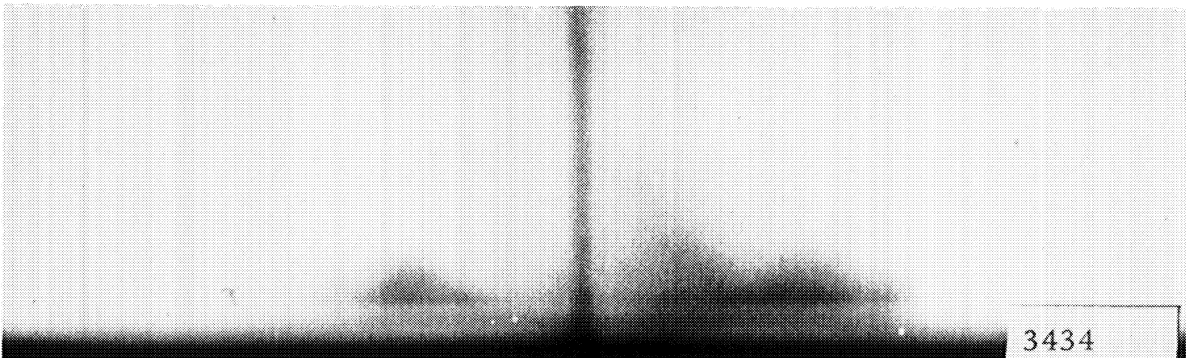
$t = 40 \, \mu s$

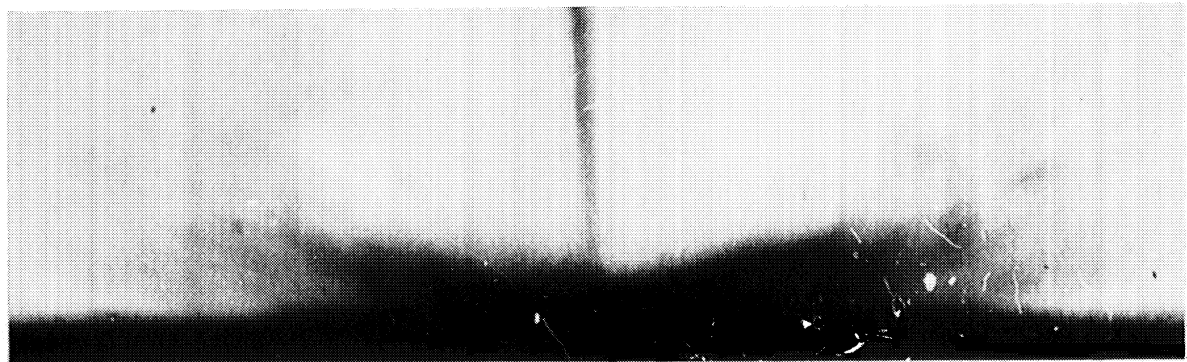Figure 4.   High-Speed Motion Picture Sequence of Jet
Impact - Goodrich #932

18

Goodrich 932

t=50 μs

t= 60 μs

t= 70 μs

3435
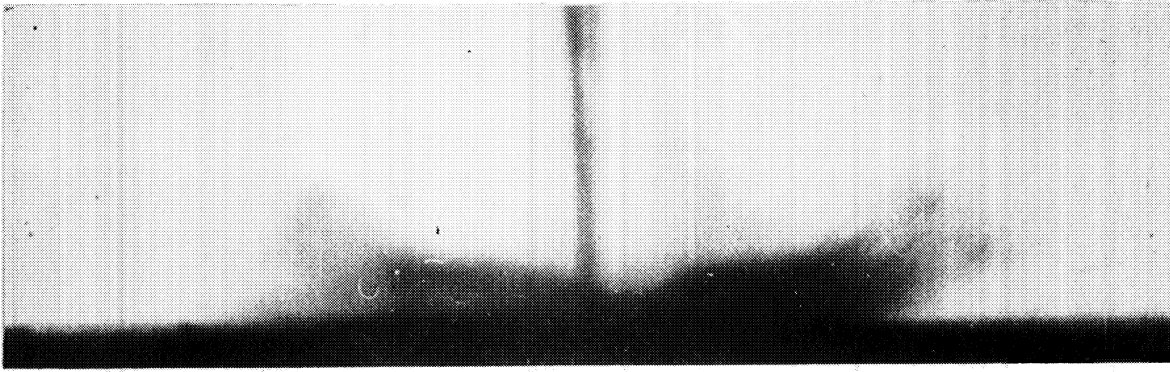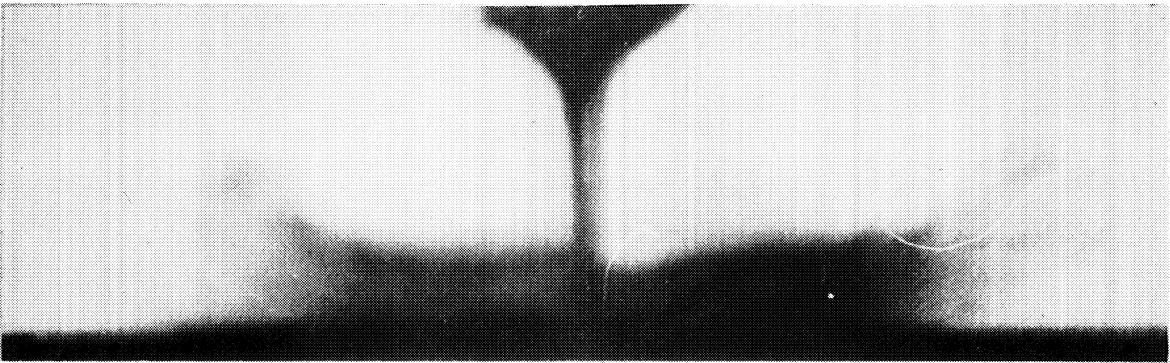
t= 80 μs

Figure 4. (Concluded)

Goodrich 936

t = 10 μs

t = 20 μs

t = 30 μs

3436
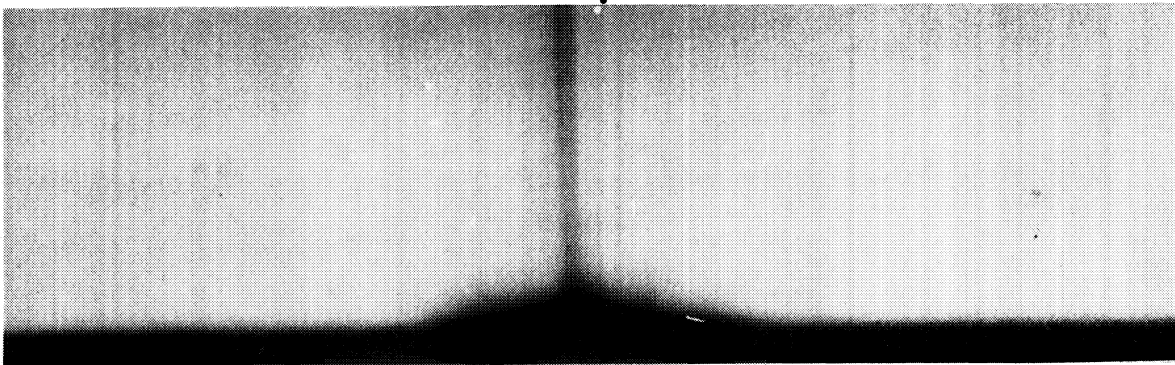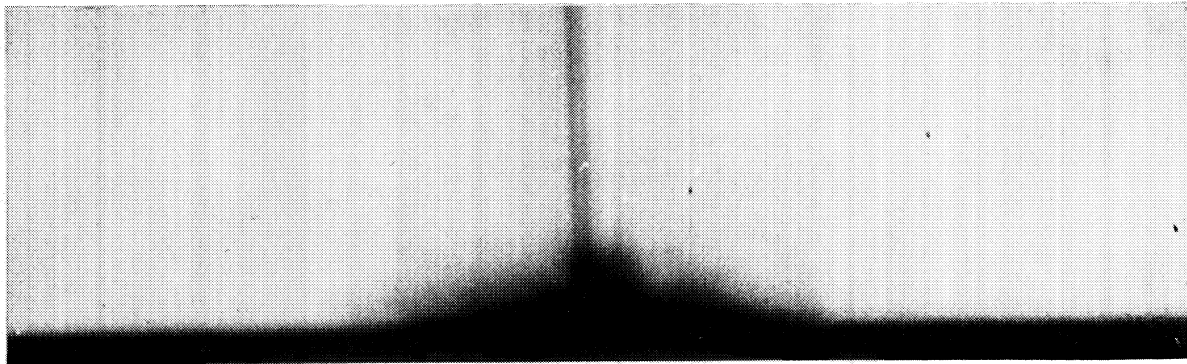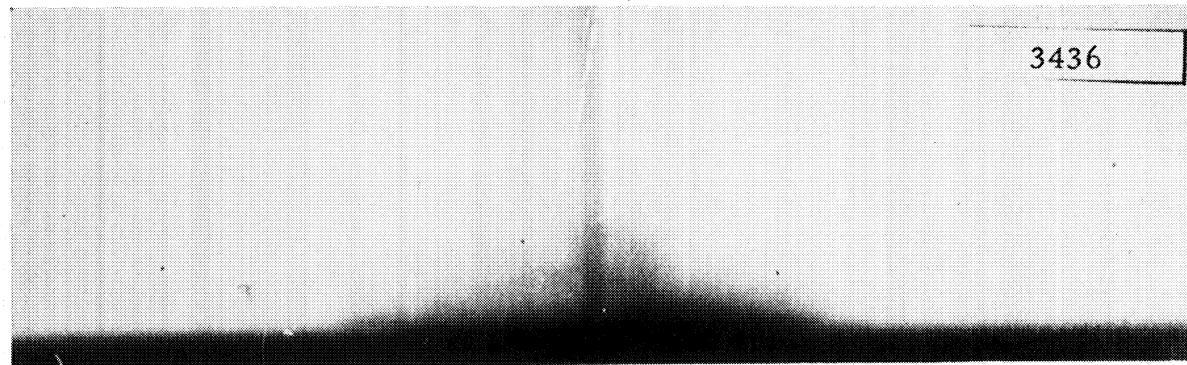
t = 40 μs

Figure 5. High-Speed Motion Picture Sequence of Jet
Impact - Goodrich #936

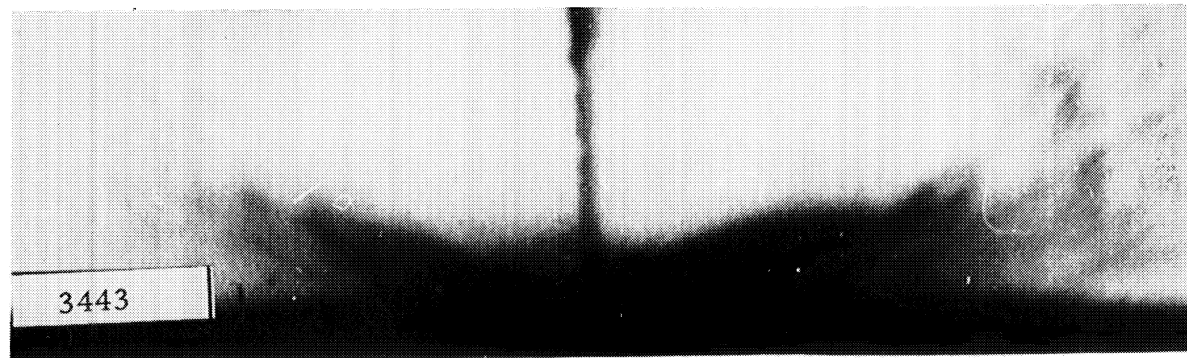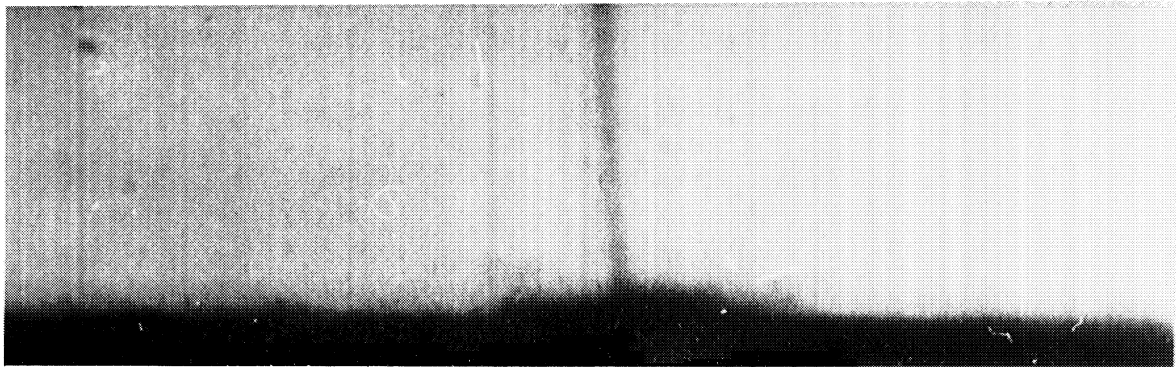# Goodrich 936
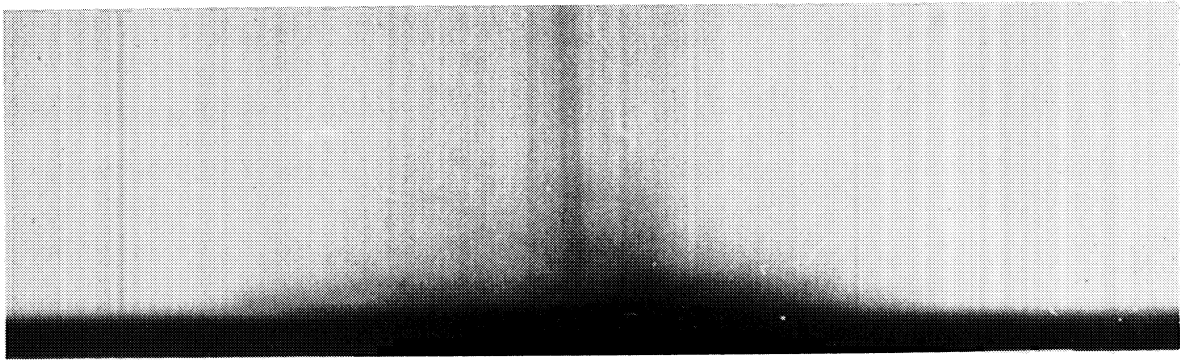
$t = 50 \, \mu s$
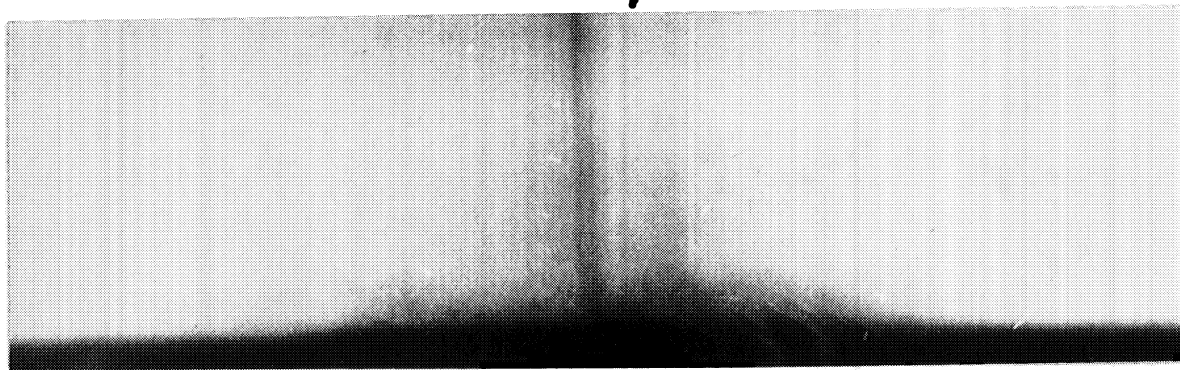
$t = 60 \, \mu s$
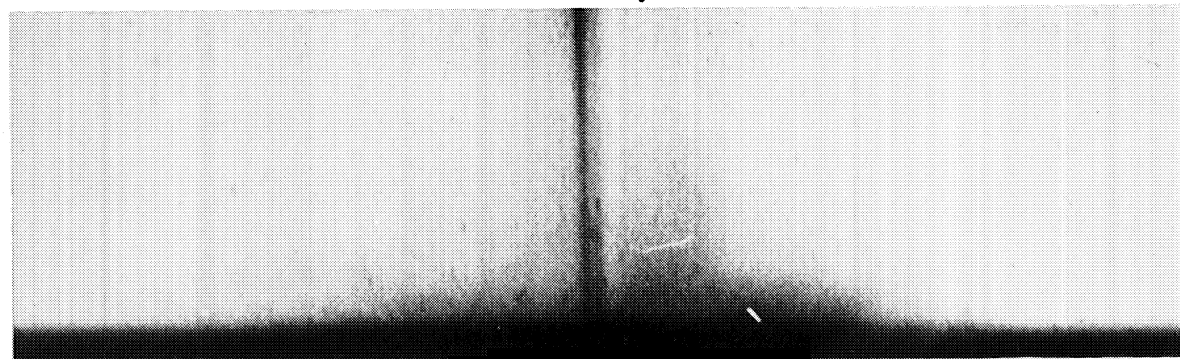
$t = 70 \, \mu s$
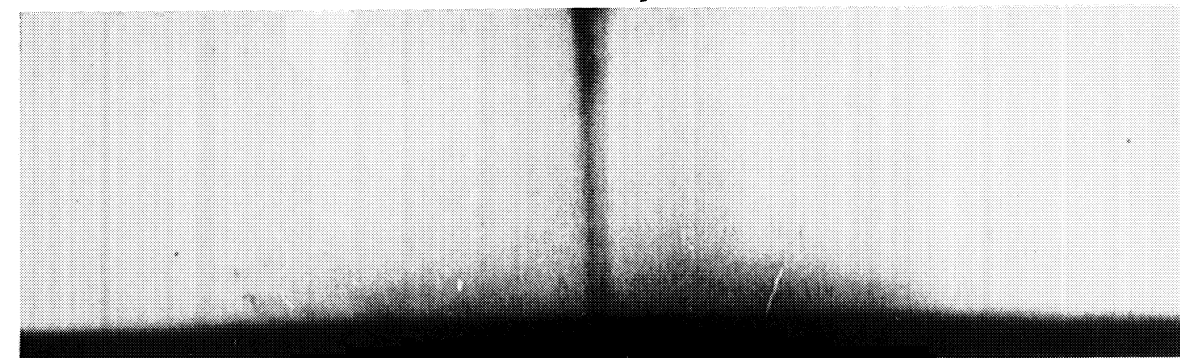
$t = 80 \, \mu s$

Figure 5. (Concluded)

Goodrich A
## WITH SCALE IN MM, IMM MEASURED ON PHOTO = .088MM,
## ALL OTHER PHOTOS TO SAME SCALE


$t = 10 \mu s$

$t = 20 \mu s$

$t = 30 \mu s$

3438
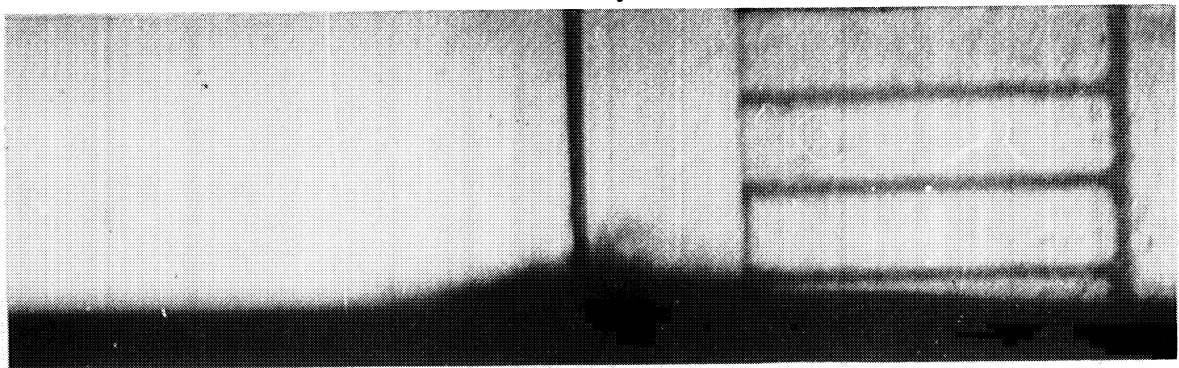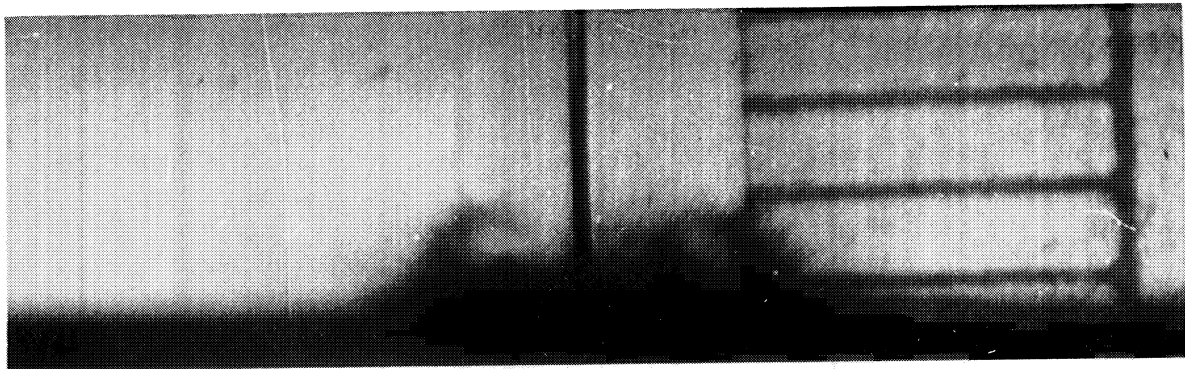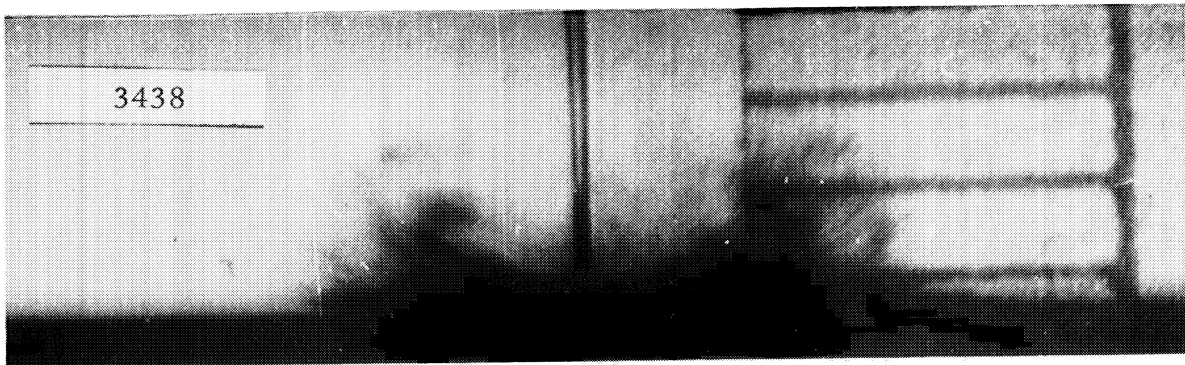
$t = 40 \mu s$

Figure 6. High-Speed Motion Picture Sequence of Jet
Impact - Goodrich #A

Goodrich A

t = 50 μs

t = 60μs

t = 70 μs

3439
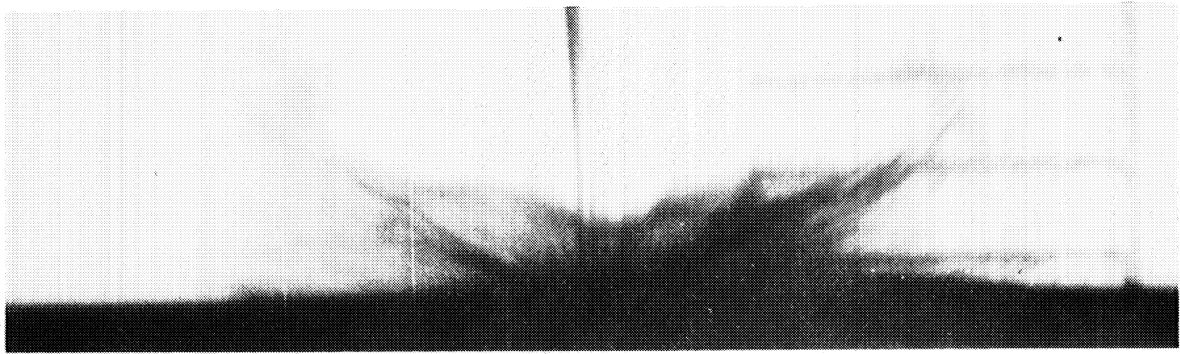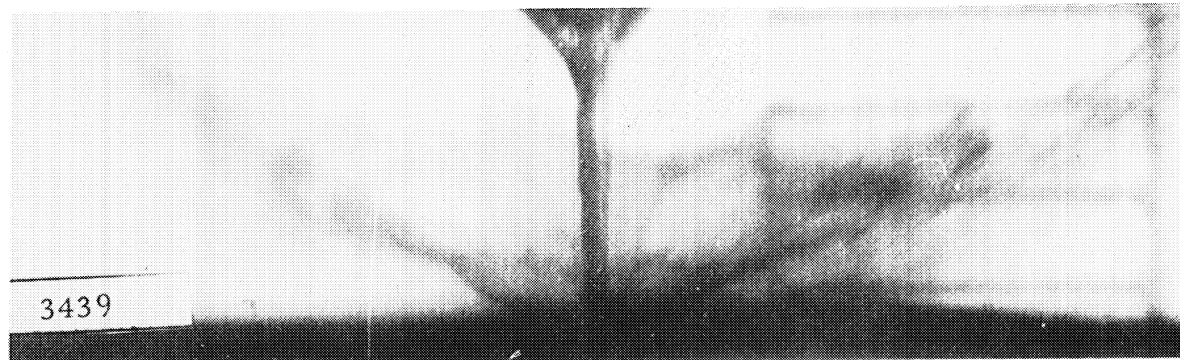
t = 80μs

Figure 6. (Concluded)

Goodrich B

t= 10 μs

t= 20 μs

t= 30 μs
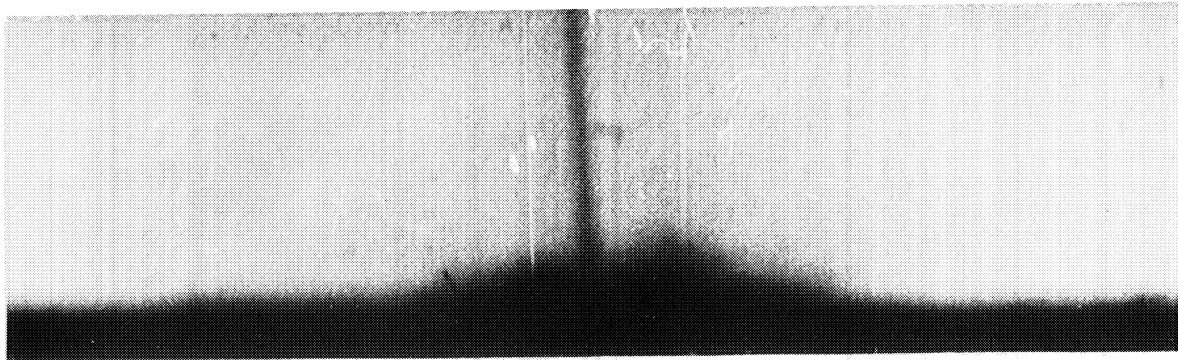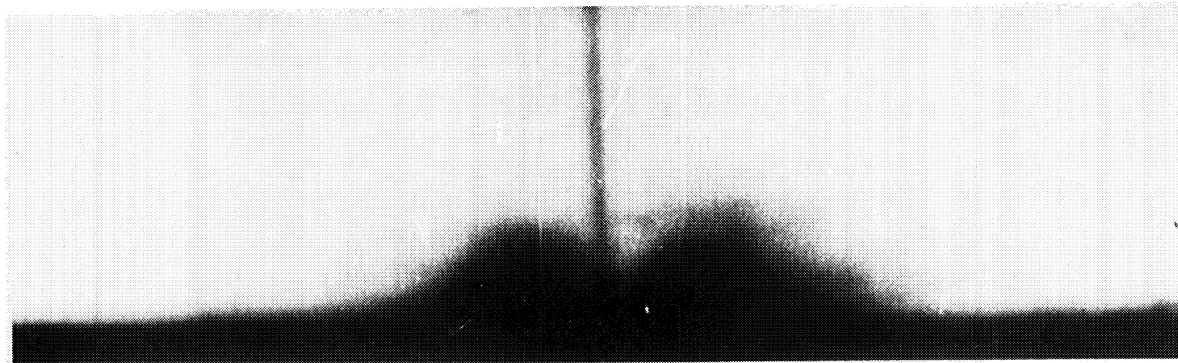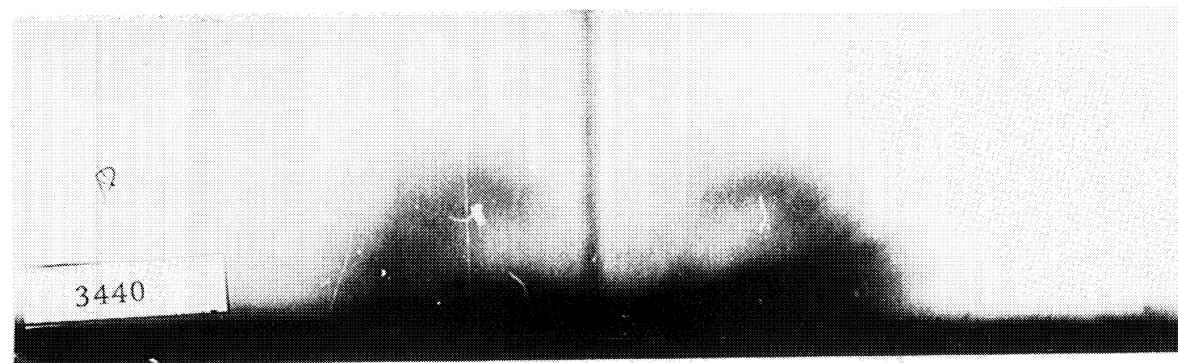
t= 40 μs

Figure 7.   High-Speed Motion Picture Sequence of Jet
Impact- Goodrich #B

Goodrich B

t= 50 μs

t= 60 μs

t= 70 μs

3441
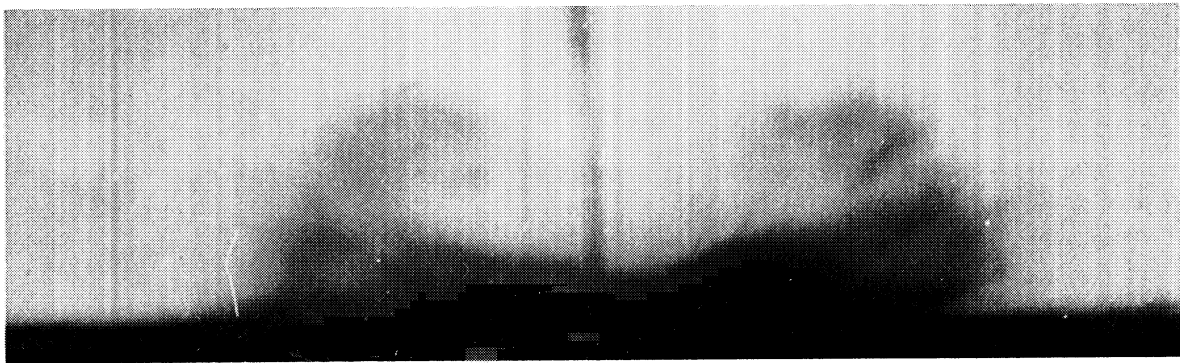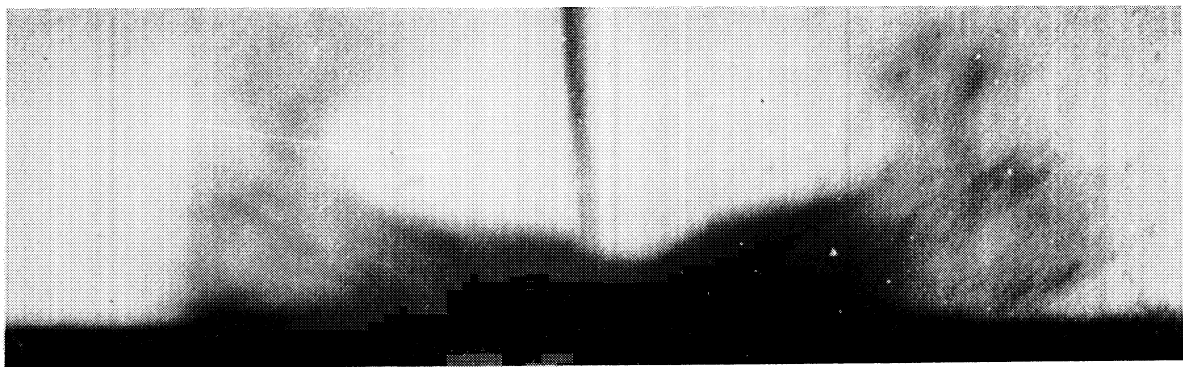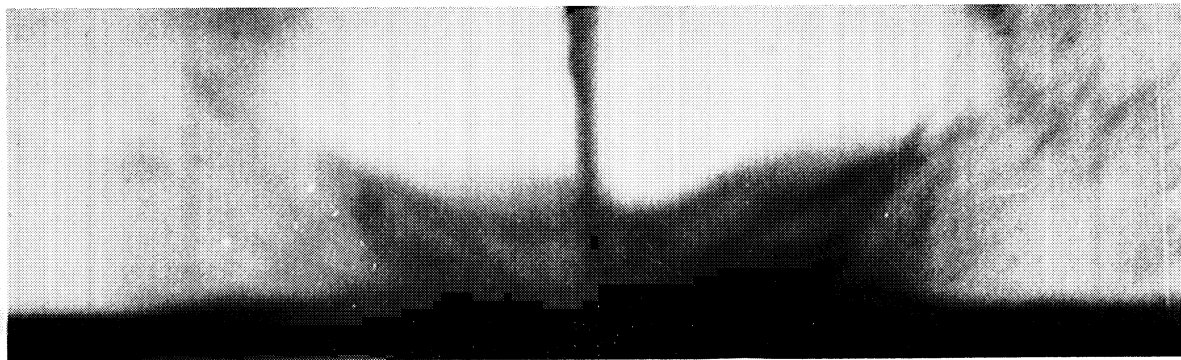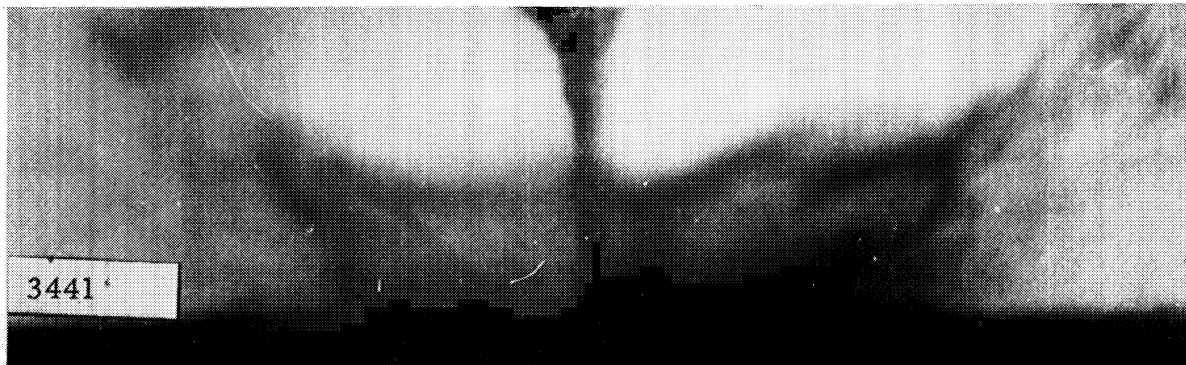
t= 80 μs

Figure 7. (Concluded)

Goodrich C
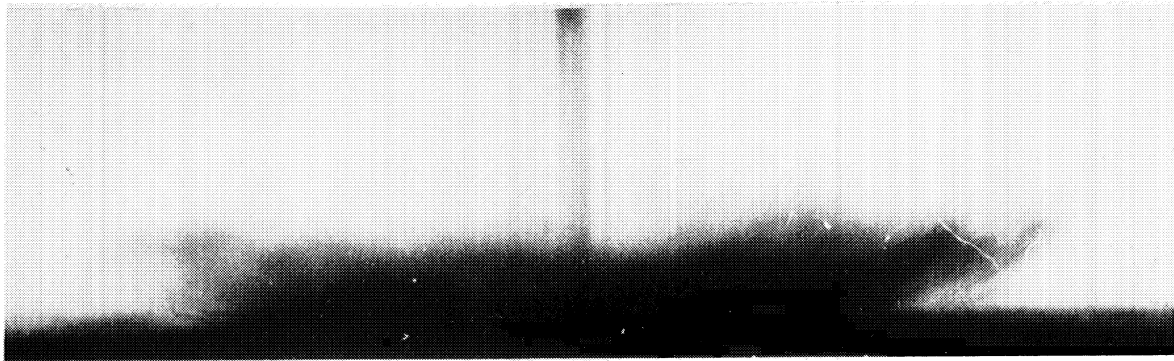

$t = 10\,\mu s$

$t = 20\,\mu s$

$t = 30\,\mu s$

3442
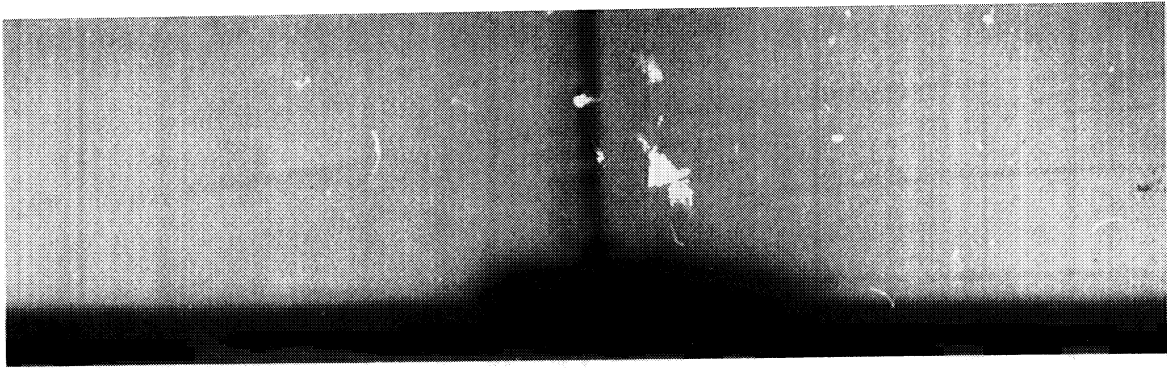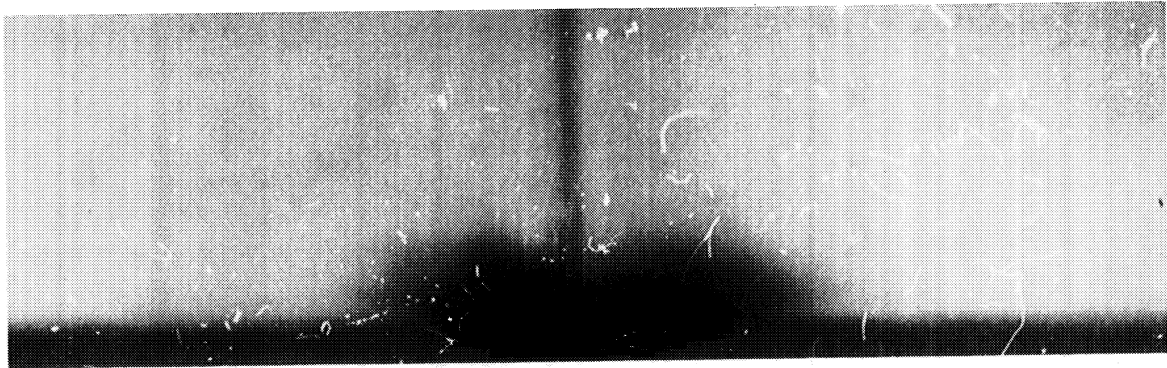
$t = 40\,\mu s$

Figure 8.   High-Speed Motion Picture Sequence of Jet
            Impact- Goodrich #C

Goodrich C

t = 50 μs

t = 60 μs

t = 70 μs

3443

t = 80 μs

Figure 8. (Concluded)

27

Goodrich D

t= 10 μs

t= 20 μs

t= 30 μs

3444
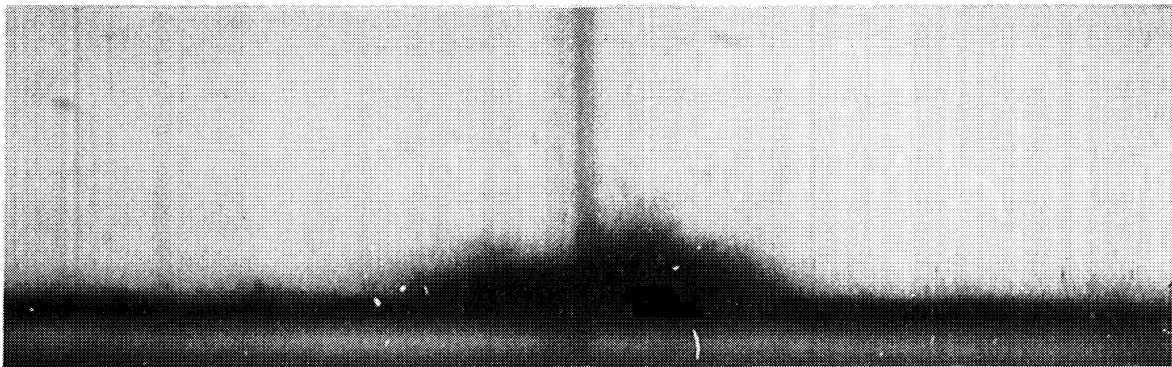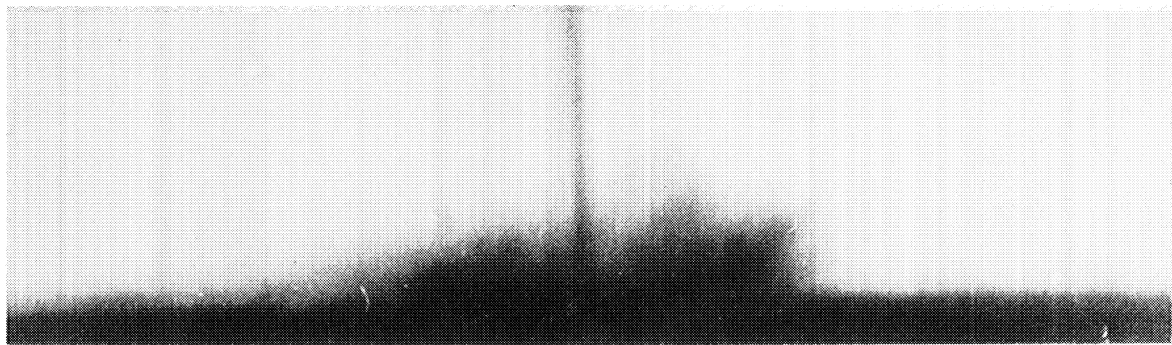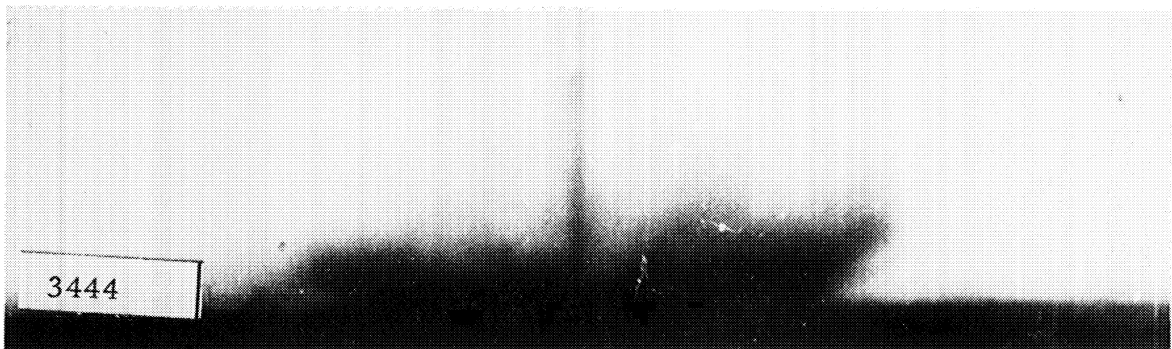
t= 40 μs

Figure 9.   High-Speed Motion Picture Sequence of Jet
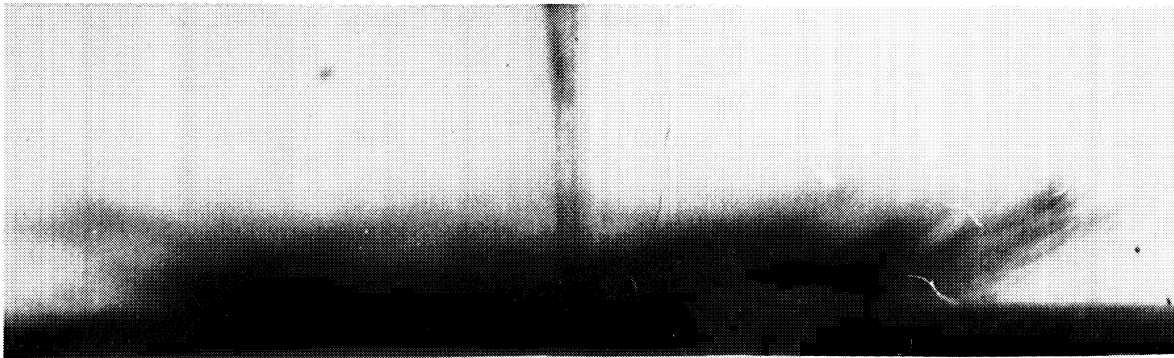Impact - Goodrich #D
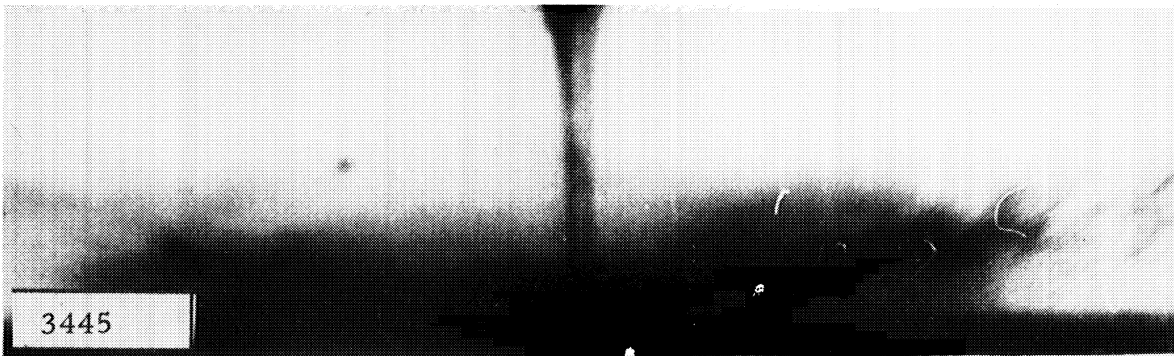
28

Goodrich D
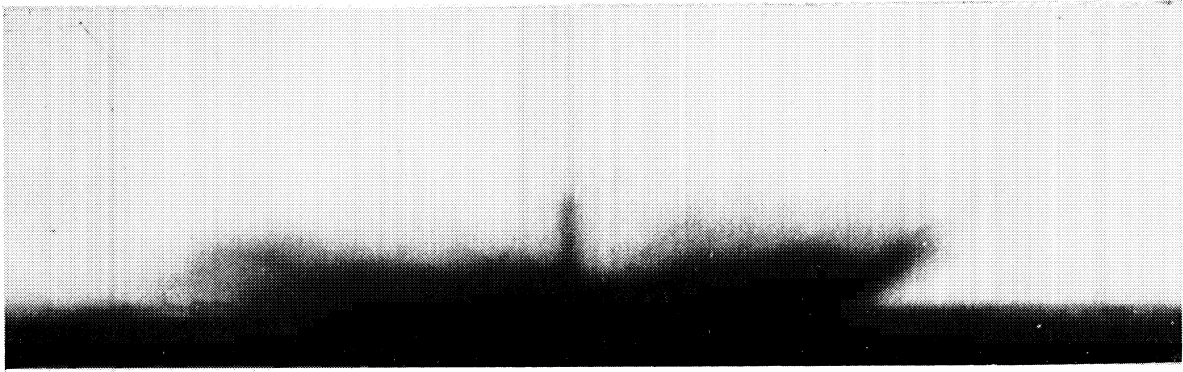
$t = 50 \, \mu s$
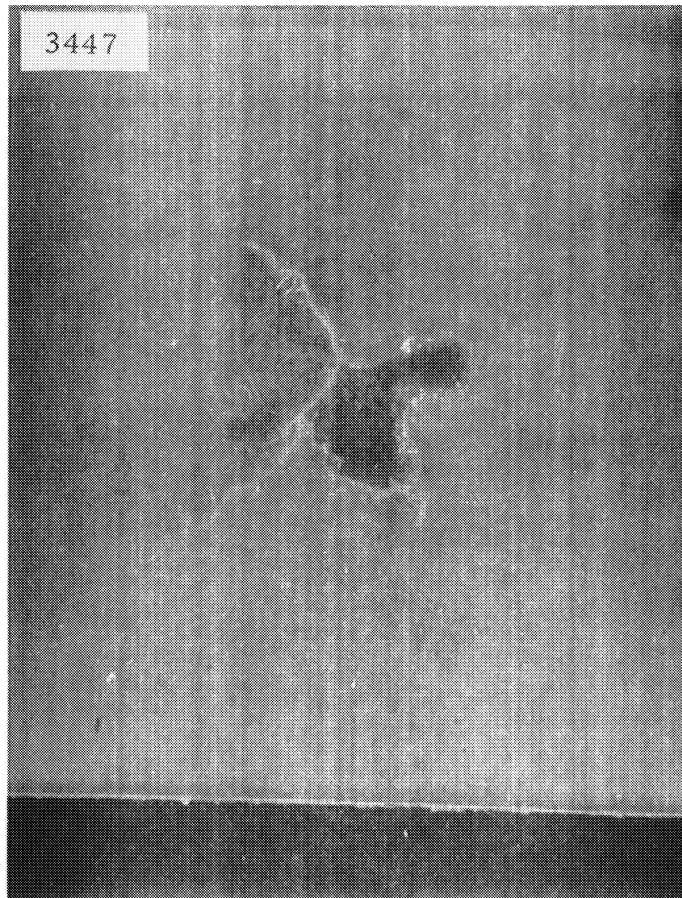
$t = 60 \, \mu s$

$t = 70 \, \mu s$

$t = 80 \, \mu s$

Figure 9. (Concluded)

(a)

(b)

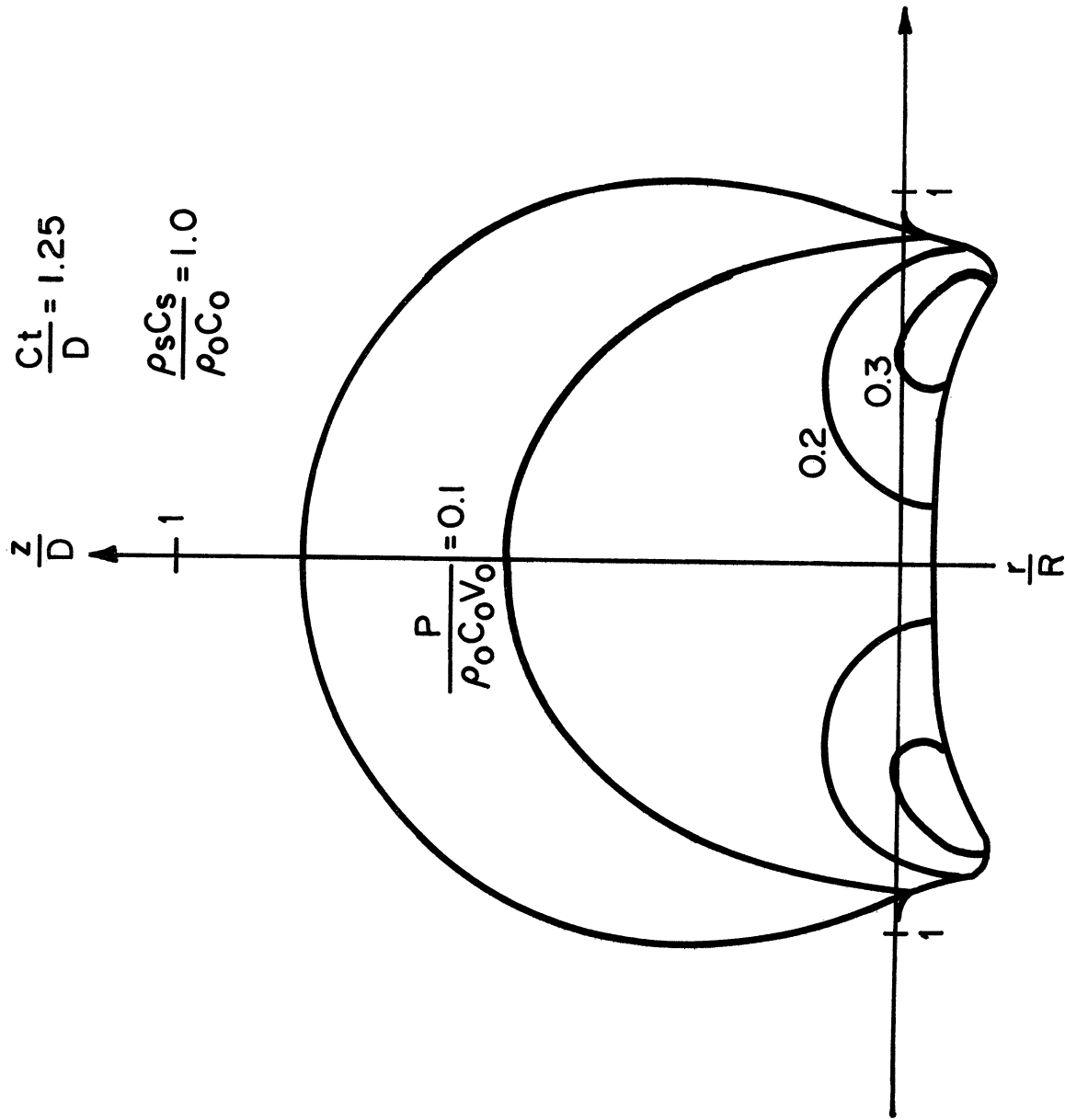16-a   Photo of Initial Failure (Specimen # 932-1)
 -b   Photo of Later Failure (Specimen #932-2)

Figure 11   Profiles for Elastic Impact

3423

31